JJMS 19, No. 2, 387-401 (2026) 387

Jordan Journal of Mathematics and Statistics.
Yarmouk University

DOI:https://doi.org/10.47013/19.2.17

A Pair of One-step Optimized Spectral Hybrid Block Methods for the Direct Solution of PDEs

Saidu Daudu Yakubu[1,6*], *Precious Sibanda*[2], *Saheed Ojo Akindeinde*[3], *Seun Evans Ogunfeyitimi*[4], *Lawal Adamu*[5]

[1] School of Mathematics, Statistics and Computer Science, University of KwaZulu-Natal, Durban, South Africa
[2] School of Mathematics, Statistics and Computer Science, University of KwaZulu-Natal, Durban, South Africa
[3] Department of Mathematics and Statistical Sciences, Botswana International University of Science and Technology, Palapye, Botswana
[4] Department of Mathematics, University of Benin, Nigeria
[5] Department of Mathematics, Federal University of Technology Minna, Nigeria
[6] Department of Mathematics, Ibrahim Badamasi Babangida University Lapai, Nigeria

Received: May 29, 2025 Accepted : Oct. 22, 2025

Abstract: This paper introduces a pair of single-step, optimized spectral hybrid block methods for the direct solution of partial differential equations. The methods are derived using an optimization approach aimed at maximizing accuracy. The methods are consistent, zero stable, convergent, and A stable. Implementation is carried out using the linear partition iteration technique, where the PDE is solved in time t using the hybrid block method and in space x using the spectral collocation method, following a suitable linear transformation. The computed results are compared with those of other numerical methods to demonstrate the efficiency and accuracy of the proposed approach. The findings indicate that the methods are both reliable and efficient.

Keywords: Spectral collocation method; Optimized hybrid block method; Linear partitioning iteration method; Partial differential equations.

2010 Mathematics Subject Classification. 35A25; 65M12; 65M70.

1 Introduction

In engineering and physics, many complex physical problems are often simplified into mathematical models that describe the underlying physical phenomena. These problems include vibrations, heat conduction, Laplace's equation, and transmission lines. In practice, such problems typically involve both spatial (x) and temporal (t) variables, leading to the formulation of partial differential equations (PDEs). Although some PDEs admit analytical solutions, many do not, prompting the development of numerical methods to approximate their solution.

To obtain numerical solutions of PDEs, various approaches have been employed. One common technique involves discretizing the first- and second-order spatial derivatives, followed by applying the method of lines to solve the resulting system of ordinary differential equations (ODEs). Biala et al. [4] developed boundary value methods (BVMs) based on linear multistep formulas to solve PDEs. Their approach transforms PDEs into second-order ODEs, which are then solved using the method of lines. In the work of Biala and Jator [2], a BVM was developed to solve three-dimensional elliptic and hyperbolic PDEs. Their method involves discretizing partial derivatives regarding two spatial variables (y,z) using finite difference approximations, reducing the PDE to a system of ODEs in the third spatial variable (x). Biala et al. [3] extended this approach by employing the Lanczos-Chebyshev reduction technique to transform second-order PDEs into second-order ODEs, which were then solved using BVM.

Motsa [13] proposed an efficient method for solving highly nonlinear boundary layer flow problems with exponentially decaying profiles. Known as the spectral local linearization method (SLLM), this technique linearizes and decouples the governing system of equations, resulting in a sequence of subsystems solved using spectral collocation methods. Other notable numerical methods include the bivariate Chebyshev spectral collocation quasilinearization method, developed

* Corresponding author e-mail: saiduyakubu2014@gmail.com;ydsaidu@ibbu.edu.ng

by Motsa et al. [14], for nonlinear evolution parabolic equations. This method integrates quasilinearization, Chebyshev spectral collocation, and bivariate Lagrange interpolation. Ramos and Rufai [17, 18] introduced one-step block hybrid methods to efficiently solve both initial value problems (IVPs) and PDEs. Liu et al. [10] proposed a sixth-order finite difference method for solving the generalized Burgers-Fisher and generalized Burgers-Huxley equations. These equations are discretized in space by a five-point sixth-order finite difference scheme combined with a truncation error modification technique and in time by the sixth-order backward difference formula to obtain solutions. Akinfe and Loyinmi [1] proposed an unrivalled hybrid scheme that involves the coupling of the new Elzaki integral transform and a modified differential transform called the projected differential transform (PDTM) for solving the generalized Burgers-Fisher's equation.

Ngwane and Jator [15] introduced an L-stable block hybrid second derivative algorithm to solve parabolic PDEs. This method is continuous and defined for all values of the independent variable, and is applied using the method of lines by approximating spatial derivatives to reduce the problem to a system of first-order IVPs. Recently, Motsa et al. [12] developed a block hybrid method for solving Lane–Emden equations, which are second-order boundary value problems with singularities at the origin. These methods utilize the quasilinearization technique.

Other recent advances in numerical analysis include the development of conformable fractional numerical methods of constant order using the fractional power series theorem, which extend classical Euler and Runge–Kutta schemes to fractional models with promising applications in finance [21]. Likewise, a unique quadratic approximation technique for the numerical evaluation of the Lambert w function has been proposed, offering high precision across real domains and improving convergence without the limitations of Newton or Halley's methods [22].

A literature review reveals that most block methods cannot solve PDEs directly; instead, the PDEs must be transformed, often resulting in increased computational cost and reduced efficiency. This study aims to address this gap by developing a pair of single-step optimized spectral hybrid block methods at different intra-step points. These methods are designed to achieve high-order accuracy, stability, and reduced computational cost for the direct solution of PDEs of the form:

$$\frac{\partial u}{\partial t} = \gamma \frac{\partial^2 u}{\partial x^2} + R(u,x,t), \quad x \in [a,b],\ 0 < t \leq T, \tag{1}$$

where $\gamma > 0$ is a diffusion coefficient and $R(u,x,t)$ is a general reaction term that may be linear, nonlinear, or zero. The initial condition is given by

$$u(x,0) = f(x), \quad x \in [a,b], \tag{2}$$

with boundary conditions

$$u(a,t) = \alpha(t), \quad u(b,t) = \beta(t), \quad 0 < t \leq T. \tag{3}$$

The present study contributes to the scope of the Jordan Journal of Mathematics and Statistics by advancing numerical and applied mathematical techniques through the development of optimized spectral hybrid block methods for efficient and accurate solutions of differential equations arising in science and engineering.

2 Development of the method

In this section, we present the derivation of a pair of single-step optimized spectral hybrid block methods for the direct numerical integration of the equation (1). It is assumed that equation (1) is well-posed and possesses a unique, continuously differentiable solution. Let $u(t)$ be a polynomial that approximates the true solution $y(t)$ of equation (1) at a set of grid points

$$y(t) \approx u(t) = \sum_{j=0}^{s+k-1} a_j t^j, \tag{4}$$

where a_j are unknown coefficients to be determined by imposing appropriate interpolation and collocation conditions on $u(t)$. The parameters s and k denote the number of interpolation points and the distinct collocation points, respectively.

To construct the method, we define the step size as $h = t_{n+1} - t_n$ over the interval $[t_n, t_{n+1}]$. Interpolation is imposed at t_n on equation (4), while the collocation conditions are applied to the derivative of equation (4) at the points t_{n+j} for $j = 0, 1$. Additional constraints are enforced at the prescribed off-step points t_{n+p_i}, where $0 < p_i < 1$ for $i = 1, 2, \ldots, m$, and m denotes the number of off-step points. The procedure is summarized as follows:

$$u(t_n) = y_n, \tag{5}$$

$$u'(t_{n+j}) = f_{n+j}, \quad j = 0, 1, \tag{6}$$

$$u'(t_{n+p_i}) = f_{n+p_i}, \quad i = 1, 2, \ldots, m. \tag{7}$$

m	Off-step points
2	$z, 1-z$
3	$z, \frac{1}{2}, 1-z$

Table 1: Number of off-step points considered.

Table 1 outlines the sets of off-step points considered in this study.
Equations (5)–(7) yield a system of $s+k$ equations whose solutions determine the coefficients a'_j, which are subsequently substituted into equation (4). After some algebraic modification, the continuous formulation of the method is obtained as:

$$u(t) = \Phi_0(t)u_n + h\left[\sum_{j=0}^{1} \chi_j(t) f_{n+j} + \sum_{i=1}^{m} \chi_{p_i}(t) f_{n+p_i}\right], \tag{8}$$

where $\Phi_0(t)$, $\chi_j(t)$, and $\chi_{p_i}(t)$ denote the continuous coefficients of the method, with $\Phi_0(t) = 1$.
Specific methods are developed by evaluating equation (8) at the appropriate off-step points. The off-step points p_i are optimized to minimize the main method's local truncation error (LTE).
Case I: Method with $m = 2$
Here, $m = 2$, and the off-step points are z and $1-z$. Expanding equation (8) using a Taylor series about t_n, the leading local truncation error becomes

$$\begin{aligned}\mathscr{L}[u(t_{n+1});h] = \frac{(5z^2-5z+1)u^{(5)}[t_n]h^5}{720} + \frac{(5z^2-5z+1)u^{(6)}[t_n]h^6}{1440} + \\ \frac{(14z^4-28z^3+77z^2-63z+12)u^{(7)}[t_n]h^7}{60480} + O(h^8).\end{aligned} \tag{9}$$

Minimizing the LTE involves setting the coefficient of h^5 to zero

$$5z^2 - 5z + 1 = 0. \tag{10}$$

Solving gives the optimized value

$$z = \frac{1}{10}(5-\sqrt{5}). \tag{11}$$

Substituting this into (9), the local truncation error reduces to

$$\mathscr{L}[u(t_{n+1});h] = \frac{h^7 u^{(7)}(t_n)}{1512000} + O(h^8). \tag{12}$$

The corresponding coefficients are provided in Table 2.

u	Φ_0	χ_0	χ_z	χ_{1-z}	χ_1
u_{n+z}	1	$\frac{11+\sqrt{5}}{120}$	$\frac{25-\sqrt{5}}{120}$	$\frac{25-13\sqrt{5}}{120}$	$\frac{-1+\sqrt{5}}{120}$
u_{n+1-z}	1	$\frac{11-\sqrt{5}}{120}$	$\frac{25+13\sqrt{5}}{120}$	$\frac{25+\sqrt{5}}{120}$	$\frac{-1-\sqrt{5}}{120}$
u_{n+1}	1	$\frac{1}{12}$	$\frac{5}{12}$	$\frac{5}{12}$	$\frac{1}{12}$

Table 2: Coefficients of the method with $m = 2$.

Case II: Method with $m = 3$
For $m = 3$, we include the midpoint $\frac{1}{2}$ among the off-step points. The leading local truncation error becomes

$$\begin{aligned}\mathscr{L}[u(t_{n+1});h] = \frac{(7z^2-7z+1)u^{(7)}[t_n]h^7}{604800} + \frac{(7z^2-7z+1)u^{(8)}[t_n]h^8}{1209600} \\ + \frac{(12z^4-24z^3+105z^2-93z+13)u^{(9)}[t_n]h^9}{58060800} + 0(h^{10}).\end{aligned} \tag{13}$$

To minimize the leading term, we set

$$7z^2 - 7z + 1 = 0, \tag{14}$$

which yields the unique solution in the range $0 < z < \frac{1}{2} < 1 - z < 1$:

$$z = \frac{1}{14}(7 - \sqrt{21}). \tag{15}$$

Substituting this into (13) reduces the LTE to

$$\mathscr{L}[u(t_{n+1});h] = -\frac{h^9 u^{(9)}(t_n)}{1422489600} + O(h^{10}). \tag{16}$$

The corresponding method coefficients are presented in Table 3.

u	Φ_0	χ_0	χ_z	$\chi_{1/2}$	χ_{1-z}	χ_1
u_{n+z}	1	$\frac{55\sqrt{21}-147}{8820(\sqrt{21}-3)}$	$\frac{7(185\sqrt{21}-609)}{8820(\sqrt{21}-3)}$	$\frac{32(85\sqrt{21}-399)}{8820(\sqrt{21}-3)}$	$\frac{7(275\sqrt{21}-1239)}{8820(\sqrt{21}-3)}$	$\frac{27(5\sqrt{21}-21)}{8820(\sqrt{21}-3)}$
$u_{n+\frac{1}{2}}$	1	$\frac{117}{2880}$	$\frac{7(15\sqrt{21}+56)}{2880}$	$\frac{512}{2880}$	$\frac{7(15\sqrt{21}-56)}{2880}$	$\frac{27}{2880}$
u_{n+1-z}	1	$\frac{9(32\sqrt{21}-102)}{4410(\sqrt{21}-3)}$	$\frac{7(34\sqrt{21}+105)}{4410(\sqrt{21}-3)}$	$\frac{16(13\sqrt{21}+105)}{4410(\sqrt{21}-3)}$	$\frac{7(79\sqrt{21}-210)}{4410(\sqrt{21}-3)}$	$\frac{-27\sqrt{21}}{4410(\sqrt{21}-3)}$
u_{n+1}	1	$\frac{9}{180}$	$\frac{49}{180}$	$\frac{64}{180}$	$\frac{49}{180}$	$\frac{9}{180}$

Table 3: Coefficients of the method with $m = 3$.

3 Theoretical analysis of the proposed schemes

In this section, the theoretical properties of the proposed schemes, constructed using m off-step points, are examined. The analysis focuses on zero-stability, convergence, linear stability, and order of accuracy. The methods can be represented in the following matrix form:

$$A_1 U_{n+1} = A_0 U_n + h(B_0 F_n + B_1 F_{n+1}), \tag{17}$$

where A_0, A_1, B_0, and B_1 are coefficient matrices of dimension $m \times m$, obtainable from Tables 2 and 3. The corresponding vectors are defined as follows:

$$\begin{aligned}
U_n &= (u_{n-p_1}, \ldots, u_{n-p_m}, u_n)^\top, \\
U_{n+1} &= (u_{n+p_1}, \ldots, u_{n+p_m}, u_{n+1})^\top, \\
F_n &= (f_{n-p_1}, \ldots, f_{n-p_m}, f_n)^\top, \\
F_{n+1} &= (f_{n+p_1}, \ldots, f_{n+p_m}, f_{n+1})^\top.
\end{aligned}$$

3.1 Order and error constants

We consider the linear difference operator $\mathscr{L}$ associated with the derived hybrid block methods, defined as

$$\mathscr{L}[u(t_n);h] = \sum_j \left[\Phi_j u(t_n + jh) - h\chi_j u'(t_n + jh)\right], \quad j = 0, p_1, p_2, \ldots, p_m, 1, \tag{18}$$

where $u(t_n)$ is a sufficiently differentiable function.
By expanding the terms $u(t_n + jh)$ and $u'(t_n + jh)$ into Taylor series about the point t_n and collecting terms according to powers of h, equation (18) becomes

$$\mathscr{L}[u(t_n);h] = C_0 u(t_n) + C_1 h u'(t_n) + \ldots + C_p h^p u^{(p)}(t_n) + C_{p+1} h^{p+1} u^{(p+1)}(t_n), \tag{19}$$

where $C_{p+1} \neq 0$.
The method with $m = 2$ has

$$C_5 = (-\frac{1}{6000\sqrt{5}}, \frac{1}{6000\sqrt{5}}, 0)^\tau,$$

indicating that the method has order $p = 4$.
Similarly, for $m = 3$, we obtain

$$C_6 = (\frac{1}{493920}, -\frac{1}{322560}, \frac{1}{493920}, 0)^\tau,$$

showing that the method has order $p = 5$.
We therefore conclude that the methods are consistent, since the order $p > 1$ for any number of off-step points (see Sunday et al. [19]).

3.2 Zero stability

To determine the zero stability of the proposed methods, we consider equation (17). Taking the limit as $h \to 0$, it reduces to

$$A_1 U_{n+1} = A_0 U_n, \tag{20}$$

where

$$A_0 = \begin{pmatrix} 0 & 0 & \dots & 1 \\ 0 & 0 & \dots & 1 \\ \vdots & \vdots & \vdots & \vdots \\ 0 & 0 & \dots & 1 \end{pmatrix}, \quad A_1 = \begin{pmatrix} 1 & 0 & \dots & 0 \\ 0 & 1 & \dots & 0 \\ \vdots & \vdots & \vdots & \vdots \\ 0 & 0 & \dots & 1 \end{pmatrix}.$$

The first characteristics polynomial $\rho(\lambda)$ is defined as

$$\rho(\lambda) = det[\lambda A_1 - A_0]. \tag{21}$$

For the single-step optimized hybrid block methods developed in this study, the characteristic polynomial simplifies to

$$\lambda^m(\lambda - 1) \; for \; m = 2, 3.$$

According to Lawal et al. [9], a numerical method is said to be zero-stable if the roots $\lambda_i, i = 1, 2, \ldots, s$ of the characteristic polynomial $\rho(\lambda)$ satisfy $|\lambda_i| \leq 1$, and any roots with $|\lambda_i| = 1$ must have multiplicity not exceeding the order of the differential equation.

Hence, the analysis confirms that the proposed methods are zero-stable. Since the methods have also been shown to be consistent, it follows by the Dahlquist Equivalence Theorem that the methods are convergent.

3.3 Region of stability

The region of stability determines where the method remains stable in the complex plane $\mathbb{C}$. To analyze the absolute stability region of the proposed methods, we apply them to the Dahlquist test equation [6], given by

$$u' = \lambda u,$$

where $\lambda \in \mathbb{C}$. Setting $q = \lambda h$, the resulting difference equation takes the form

$$U_{n+1} = M(q) U_n, \tag{22}$$

where the matrix $M(q)$ is defined as

$$M(q) = (A_1 - qB_1)^{-1}.(A_0 + qB_0),$$

and is referred to as the amplification matrix.
The spectral radii for the methods with different values of m are given below:
For $m = 2$, we obtain

$$\rho(q) = \frac{-q - 12}{q - 12}.$$

For $m = 3$, we have

$$\rho(q) = \frac{q^2 + 41q + 180}{q^2 + 41q - 180}.$$

The stability regions corresponding to the methods with $m = 2$ and $m = 3$ are shown in Figures 1a and 1b. These plots illustrate that the methods possess identical stability regions.

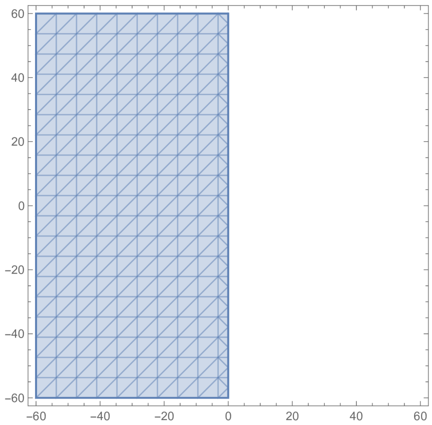

(a) Stability region of the method with $m = 2$

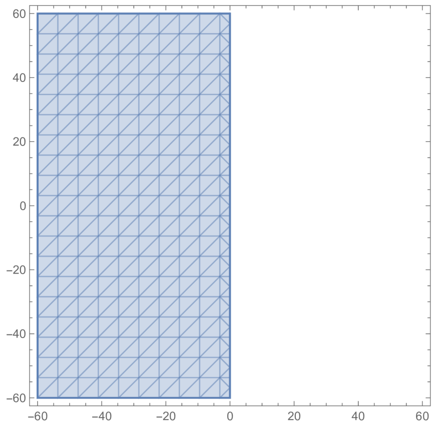

(b) Stability region of the method with $m = 3$

Fig. 1: Stability regions of the methods in Tables 2 and 3.

A numerical method is said to be A-stable if its region of absolute stability includes the entire left half of the complex plane $\mathbb{C}$ (see Lambert [8]). Therefore, both methods are A-stable.

4 Implementation of the methods

In this section, we describe the implementation of the proposed hybrid block methods for solving equation (1). We adopt the Linear Partitioning Iteration Method (LPIM), which is a Newton-Raphson-type iterative procedure used to linearize nonlinear problems. The resulting system is then integrated using the hybrid block approach. The methods were implemented in MATLAB R2022b on an HP 15s-fq4015ni system running Windows 11, equipped with an Intel Core i5-1155G7 processor, 16 GB RAM, and a 515 GB solid-state drive (SSD).
Note that the methods developed for $m = 2$ and $m = 3$ are denoted as OSHBM1 and OSHBM2, respectively.

4.1 Transformation

The physical domain $t \in [0, T]$ is transformed to the standard domain $\hat{t} \in [-1, 1]$ via the linear mapping:

$$t = \frac{T(\hat{t} + 1)}{2}.$$

Similarly, the spatial domain $x \in [a, b]$ is mapped to $\hat{x} \in [-1, 1]$ using

$$x = \frac{(b-a)}{2}\hat{x} + \frac{(b+a)}{2}.$$

The continuous spatial derivatives are discretized using the Chebyshev spectral collocation method. This involves constructing Chebyshev differentiation matrices to approximate the spatial derivatives as

$$\frac{\partial u}{\partial x}(x_i, t) \to DU(t), \; \frac{\partial^2 u}{\partial x^2}(x_i, t) \to D^2U(t),$$

where D is the Chebyshev differentiation matrix as defined by Trefethen [20], and

$$U(t) = [u(x_0,t), u(x_1,t), \ldots, u(x_{N_x},t)]^{\tau}.$$

The spatial collocation points are chosen as Gauss–Lobatto points on the interval $[-1,1]$, given by

$$x_i = \cos\left(\frac{\pi_i}{N_x}\right), i = 0, 1, \ldots, N_x.$$

After applying the spectral collocation method in space, the optimized hybrid block method takes the form

$$U_{n+p_i} = U_n + h\sum_{j=0}^{m} \beta_{i,j} F_{n+p_i}, \quad i = 1, 2, \ldots, m, \tag{23}$$

where

$$U_{n+p_i} = [u(x_0,t_{n+p_i}), u(x_1,t_{n+p_i}), \ldots, u(x_{N_x},t_{n+p_i})]^{\tau},$$

and

$$F_{n+p_i} = f\left(t_{n+p_i}, U_{n+p_i}\right).$$

4.2 Linear partitioning iteration method (LPIM)

To implement the hybrid block methods, we apply the linear partitioning iteration method based on equation (23). The nonlinear function $f(t,u)$ is partitioned into linear and nonlinear components as follows

$$f(t,u) = \mathscr{L}(t,u,u',u'') + \mathscr{N}(t,u,u',u''), \tag{24}$$

where $\mathscr{L}$ represents the linear part, and $\mathscr{N}$ captures the remaining nonlinear terms. The iterative scheme is formulated as

$$U^{(r+1)}_{n+p_i} = U_n + h\sum_{j=0}^{m} \beta_{i,j} F^{(r+1)}_{n+p_i}, \tag{25}$$

which, upon substitution of the partitioned components, becomes

$$U^{(r+1)}_{n+p_i} = U_n + h\sum_{j=0}^{m} \beta_{i,j}\left[\mathscr{L}(t_{n+p_j})U^{(r+1)}_{n+p_j} + \mathscr{N}(t_{n+p_j}, U^{(r)}_{n+p_j})\right]. \tag{26}$$

Here, the linear terms are evaluated at the current iteration level $(r+1)$, while the nonlinear terms are evaluated at the previous iteration level (r). Rearranging equation (26) yields:

$$U^{(r+1)}_{n+p_i} - h\sum_{j=1}^{m} \beta_{i,j}\mathscr{L}\left(t_{n+p_j}\right)U^{(r+1)}_{n+p_j} = U_n + h\beta_{i,0}F_n + h\sum_{j=1}^{m} \beta_{i,j}\mathscr{N}\left(t_{n+p_j}, U^{(r)}_{n+p_j}\right). \tag{27}$$

This system can be expressed compactly using the Kronecker product as

$$(\mathbf{I} - h(A\otimes I)\mathscr{L}_{n+p})\mathbf{U}^{(r+1)}_{n+p} = \mathbf{U}_n + h(A_0\otimes I)\mathbf{F}_n + h(A\otimes I)\mathscr{N}^{(r)}_{n+p}, \tag{28}$$

where I is the $(N_x+1)\times(N_x+1)$ identity matrix, $\mathbf{I}$ is the $m(N_x+1)\times m(N_x+1)$ identity matrix, $\mathbf{U}_n$ and $\mathbf{F}_n$ are vectors of size $m(N_x+1)\times 1$, defined as

$$\mathbf{F}_n = \begin{bmatrix} F_n \\ F_n \\ \vdots \\ F_n \end{bmatrix}, \quad \mathbf{U}_n = \begin{bmatrix} U_n \\ U_n \\ \vdots \\ U_n \end{bmatrix},$$

and

$$A_0 = \begin{bmatrix} \beta_{1,0} & 0 & \dots & 0 \\ 0 & \beta_{2,0} & \dots & 0 \\ \vdots & \vdots & \dots & \vdots \\ 0 & 0 & \dots & \beta_{m,0} \end{bmatrix}, \quad A = \begin{bmatrix} \beta_{1,1} & \beta_{1,2} & \cdots & \beta_{1,m} \\ \beta_{2,1} & \beta_{2,2} & \cdots & \beta_{2,m} \\ \vdots & \vdots & \vdots & \vdots \\ \beta_{m,1} & \beta_{m,2} & \cdots & \beta_{m,m} \end{bmatrix},$$

$$\mathscr{L}_{n+p}^{(r+1)} = \begin{bmatrix} \mathscr{L}(t_{n+p_1}) & 0 & \dots & 0 \\ 0 & \mathscr{L}(t_{n+p_2}) & \dots & 0 \\ \vdots & \vdots & \dots & \vdots \\ 0 & 0 & \dots & \mathscr{L}(t_{n+p_m}) \end{bmatrix}, \quad \mathscr{N}_{n+p}^{(r)} = \begin{bmatrix} \mathscr{N}\left(t_{n+p_1}, U_{n+p_1}^{(r)}\right) \\ \mathscr{N}\left(t_{n+p_2}, U_{n+p_2}^{(r)}\right) \\ \vdots \\ \mathscr{N}\left(t_{n+p_m}, U_{n+p_m}^{(r)}\right) \end{bmatrix}.$$

The pseudocode outlining the implementation of the LPIM-based Hybrid Block Method is presented below.

Step 1.Domain Transformation: Map the physical domains to the standard interval:

$$t = \frac{T(\hat{t}+1)}{2}, \qquad x = \frac{(b-a)}{2}\hat{x} + \frac{(b+a)}{2}.$$

Step 2.Spatial Discretization: Apply Chebyshev spectral collocation:

$$\frac{\partial u}{\partial x} \approx DU(t), \qquad \frac{\partial^2 u}{\partial x^2} \approx D^2 U(t),$$

where D is the Chebyshev differentiation matrix at Gauss–Lobatto points $x_i = \cos\left(\frac{\pi i}{N_x}\right)$.

Step 3.Temporal Discretization: Adopt the optimized hybrid block formulation:

$$U_{n+p_i} = U_n + h\sum_{j=0}^{m} \beta_{i,j} F_{n+p_j}, \quad F_{n+p_j} = f(t_{n+p_j}, U_{n+p_j}).$$

Step 4.Linear Partitioning of the Nonlinear Term: Decompose $f(t,u)$ into linear and nonlinear parts:

$$f(t,u) = \mathscr{L}(t,u,u',u'') + \mathscr{N}(t,u,u',u'').$$

Step 5.Iterative Linearization (LPIM): At iteration level r, evaluate linear terms at $(r+1)$ and nonlinear terms at (r):

$$U_{n+p_i}^{(r+1)} = U_n + h\sum_{j=0}^{m} \beta_{i,j}\left[\mathscr{L}(t_{n+p_j})U_{n+p_j}^{(r+1)} + \mathscr{N}(t_{n+p_j}, U_{n+p_j}^{(r)})\right].$$

Step 6.Matrix Formulation: Assemble the coupled block system:

$$(\mathbf{I} - h(A\otimes I)\mathscr{L}_{n+p})\mathbf{U}_{n+p}^{(r+1)} = \mathbf{U}_n + h(A_0\otimes I)\mathbf{F}_n + h(A\otimes I)\mathscr{N}_{n+p}^{(r)}.$$

Step 7.Iterative Solution: Solve for $\mathbf{U}_{n+p}^{(r+1)}$ until

$$\|\mathbf{U}_{n+p}^{(r+1)} - \mathbf{U}_{n+p}^{(r)}\|_\infty < \varepsilon_{\text{tol}}.$$

If convergence fails, reduce h or increase the iteration limit.

Step 8.Block Advancement: Update U_{n+1} from the accepted block solution and proceed to the next block.

Step 9.Postprocessing: Recover $u(x,t)$ on the physical domain and compute diagnostic quantities (errors, norms, etc.).

The PDEs are efficiently solved using the hybrid block method in the temporal domain t, combined with the spectral collocation method in the spatial domain x.

5 Results and discussion

In this section, we present numerical results obtained by applying the proposed methods to selected test problems to assess their performance and accuracy.
The maximum absolute error is computed as

$$\max\left|u_{i,j}-u(x_i,t_j)\right|, \quad 0\le i\le m, \quad 0\le j\le N, \tag{29}$$

where u_{ij} denotes the numerical approximation of the exact solution $u(x_i,t_j)$ at the mesh point (x_i,t_j).

Problem 1
Consider the PDE studied in [5, 15]

$$\frac{\partial u}{\partial t}=K\frac{\partial^2 u}{\partial x^2}, \quad x\in[0,1], \quad t>0, \tag{30}$$

with the boundary conditions: $u(0,t)=u(1,t)=0$, and initial condition $u(x,0)=\sin\pi x$.
The exact solution is

$$u(x,t)=e^{-\pi^2 Kt}\sin\pi x.$$

Problem 2
Consider the stiff parabolic PDE solved by Ngwane and Jator [5, 15]

$$\frac{\partial u}{\partial t}=K\frac{\partial^2 u}{\partial x^2}, \quad x\in[0,1], \quad t>0, \tag{31}$$

with the boundary conditions: $u(0,t)=u(1,t)=0$, and initial condition $u(x,0)=\sin\pi x+\sin\omega\pi x, \quad \omega\ge 1$.
The exact solution is $u(x,t)=e^{-\pi^2 Kt}\sin\pi x+e^{-\omega^2\pi^2 Kt}\sin\omega\pi x$.
Problem 3

Consider the Fisher–KPP equation studied in [7, 11, 14]

$$\frac{\partial u}{\partial t}=\frac{\partial^2 u}{\partial x^2}-u(1-u)(\rho-u), \quad x\in[-1,1], \quad t>0, \tag{32}$$

with boundary and initial conditions:
$u(-1,t)=\frac{1}{2}+\frac{1}{2}\tanh\left(\frac{-1}{2\sqrt{2}}-\frac{(2\rho-1)t}{4}\right)$,
$u(1,t)=\frac{1}{2}+\frac{1}{2}\tanh\left(\frac{1}{2\sqrt{2}}-\frac{(2\rho-1)t}{4}\right)$,
$u(x,0)=\frac{1}{2}+\frac{1}{2}\tanh\left(\frac{x}{2\sqrt{2}}\right)$.

The exact solution is

$$u(x,t)=\frac{1}{2}+\frac{1}{2}\tanh\left(\frac{x}{2\sqrt{2}}-\frac{(2\rho-1)t}{4}\right).$$

Problem 4
Consider the standard heat equation [16]

$$\frac{\partial u}{\partial t}=\frac{\partial^2 u}{\partial x^2}, \quad x\in(0,\pi), \quad t>0, \tag{33}$$

with the boundary and initial conditions: $u(0,t)=u(\pi,t)=0, \quad u(x,0)=\sin x$.
The exact solution is $u(x,t)=e^{-t}\sin x$.

h	K	OSHBM1	OSHBM2	BHSDA [15]	Cash [5] (2.6a,b)
0.1	1	4.8603×10^{-9}	1.8615×10^{-11}	1.3000×10^{-6}	1.5000×10^{-5}
0.05	1	7.3833×10^{-11}	7.1187×10^{-14}	1.7000×10^{-7}	4.0000×10^{-6}

Table 4: Comparison of absolute errors at $t=1$ for Problem 1.

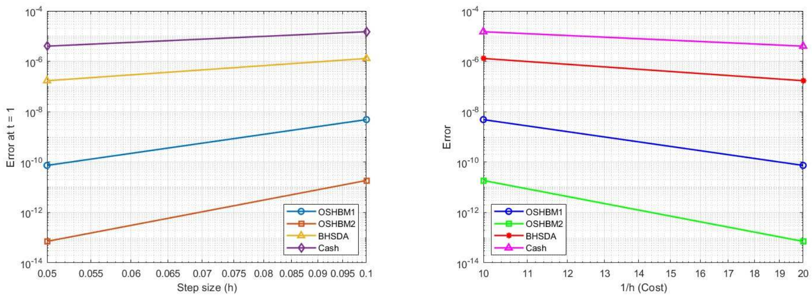

(a) Absolute error **(b)** Efficiency

Fig. 2: Error graph at $t = 1$ for Problem 1.

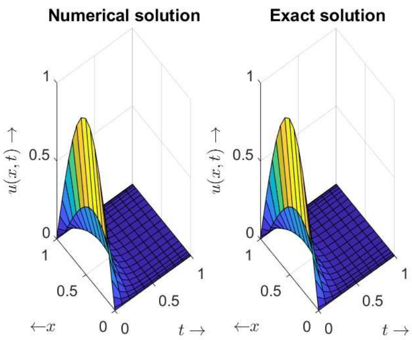

Fig. 3: Solution graph for Problem 1.

Table 4 presents the absolute errors for various numerical methods at the final time $t = 1$, using different step sizes (h) for problem 1. The graphical results shown in Figure 3 illustrate the close agreement between the numerical and exact solutions obtained using OSHBM1 and OSHBM2. It is evident from Table 4 that OSHBM1 and OSHBM2 outperform the other methods, despite having the same order, thereby demonstrating their efficiency and accuracy.

ω	BHSDA [15]	Cash [5] (2.6a,b)	OSHBM1	OSHBM2
1	2.6400×10^{-6}	3.7200×10^{-5}	9.7207×10^{-9}	3.7229×10^{-11}
2	1.3200×10^{-6}	1.8000×10^{-5}	4.8603×10^{-9}	1.8615×10^{-11}
3	1.3200×10^{-6}	1.9000×10^{-5}	4.8644×10^{-9}	1.8614×10^{-11}
5	1.3200×10^{-6}	1.8000×10^{-5}	6.1674×10^{-5}	1.0329×10^{-7}

Table 5: Comparison of absolute errors at $t = 1$, $K = 1$, and $h = 0.1$ for Problem 2.

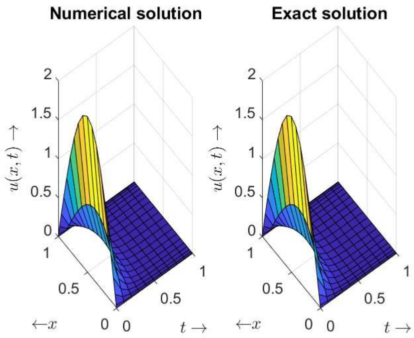

Fig. 4: Solution graph for Problem 2.

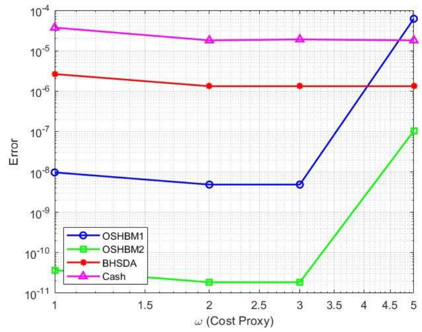

Fig. 5: Efficiency curve for Problem 2.

Table 5 presents a comparison of the absolute errors at $t = 1$ for Problem 2 for various values of ω. Figure 4 shows the graphical results, confirming that the numerical results produced by OSHBM1 and OSHBM2 closely match the exact solution. The results presented in Figure 5 demonstrate the superior performance of OSHBM1 and OSHBM2 over the existing methods, highlighting the robustness and accuracy of the new techniques.

t	OSHBM1 NFE = 190, CPU Time = 0.0115	OSHBM2 NFE = 250, CPU Time = 0.0117
0.1	2.3226×10^{-13}	6.8834×10^{-15}
0.2	2.6679×10^{-13}	4.7740×10^{-15}
0.3	3.3734×10^{-13}	4.4409×10^{-15}
0.4	4.0012×10^{-13}	5.2180×10^{-15}
0.5	4.5730×10^{-13}	6.1062×10^{-15}
0.6	5.2197×10^{-13}	8.8818×10^{-15}
0.7	5.7482×10^{-13}	1.0214×10^{-14}
0.8	6.3277×10^{-13}	1.4322×10^{-14}
0.9	6.8112×10^{-13}	1.3101×10^{-14}
1.0	7.3130×10^{-13}	1.2879×10^{-14}

Table 6: Comparison of absolute errors for Problem 3 using $h = 0.1$ and $\rho = 0.1$.

N	OSHBM1	NFE	CPU Time	OSHBM2	NFE	CPU Time
20	2.7291×10^{-12}	190	0.0115	3.6054×10^{-14}	250	0.0117
40	3.8133×10^{-12}	190	0.0340	6.4230×10^{-14}	250	0.0381
60	4.7624×10^{-12}	190	0.0467	3.6455×10^{-13}	250	0.0526
80	5.5933×10^{-12}	190	0.0568	3.5375×10^{-13}	250	0.0815
100	5.9538×10^{-12}	190	0.0754	1.3659×10^{-12}	250	0.1662

Table 7: Maximum errors of methods for Problem 3 using $h = 0.1$ and $\rho = 0.1$.

Table 6 shows the absolute errors at various time points for Problem 3 using OSHBM1 and OSHBM2 with $h = 0.1$ and $\rho = 0.1$. The results are presented at the collocation point $N = 20$. The table also presents the number of function evaluations (NFE) and CPU time for both methods. OSHBM2 yields smaller absolute errors compared to OSHBM1, demonstrating its superior accuracy.

Table 7 presents the maximum absolute errors for OSHBM1 and OSHBM2 at different values of N, representing the number of collocation points. As observed, increasing N leads to a reduction in error at the cost of increased CPU time. Figure 6 compares the errors of OSHBM1 and OSHBM2, illustrating their respective performances with $h = 0.1$, while Figure 7 displays the graphical solution for Problem 3.

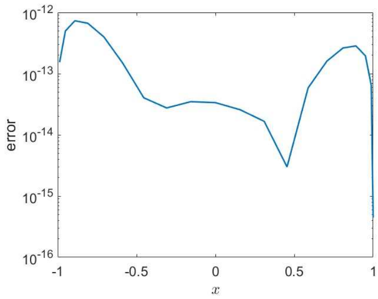

(a) Error of OSHBM1

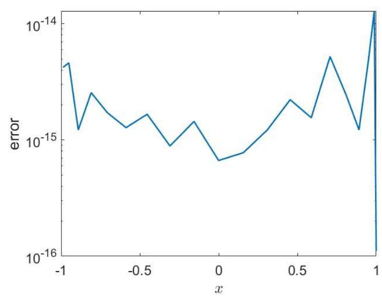

(b) Error of OSHBM2

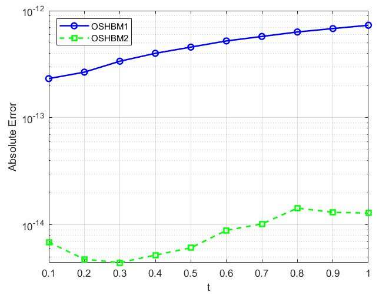

(c) Absolute error

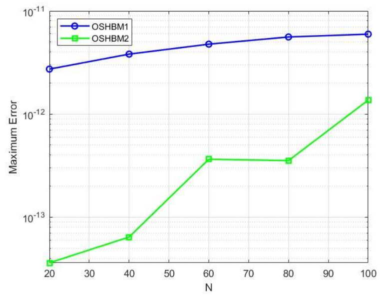

(d) Maximum error

Fig. 6: Errors graph for Problem 3.

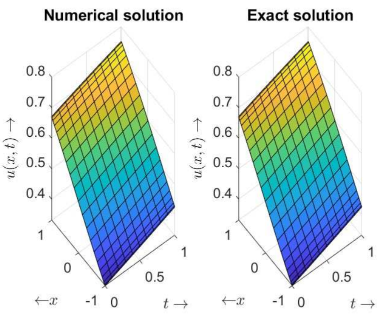

(a) Numerical vs Exact

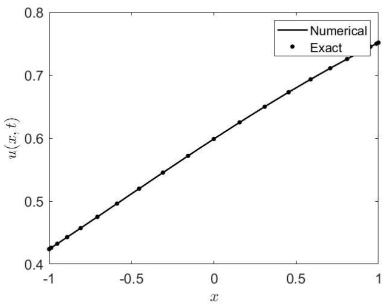

(b) Solution profile of OSHBM1&2

Fig. 7: Solution graph for Problem 3.

t	OSHBM1 NFE = 130, CPU Time = 0.0242	OSHBM2 NFE = 170, CPU Time = 0.0245
0.1	8.9839×10^{-13}	2.3315×10^{-15}
0.2	1.6250×10^{-12}	2.9976×10^{-15}
0.3	2.2050×10^{-12}	3.6637×10^{-15}
0.4	2.6601×10^{-12}	4.3299×10^{-15}
0.5	3.0087×10^{-12}	4.4409×10^{-15}
0.6	3.2665×10^{-12}	4.3299×10^{-15}
0.7	3.4481×10^{-12}	4.7184×10^{-15}
0.8	3.5658×10^{-12}	4.7740×10^{-15}
0.9	3.6297×10^{-12}	4.7184×10^{-15}
1.0	3.6491×10^{-12}	4.7184×10^{-15}

Table 8: Comparison of absolute errors for Problem 4 using $h = 0.1$.

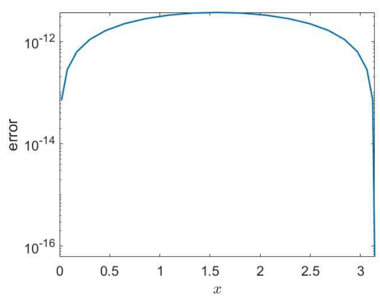

(a) Error of OSHBM1

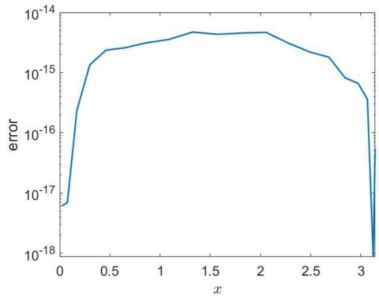

(b) Error of OSHBM2

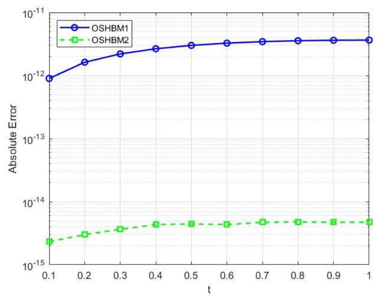

(c) Absolute error

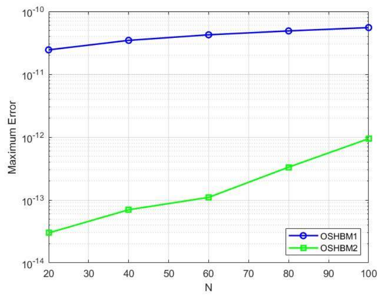

(d) Maximum error

Fig. 8: Errors graph for Problem 4.

N	OSHBM1	NFE	CPU Time	OSHBM2	NFE	CPU Time
20	2.4486×10^{-11}	130	0.0242	2.9998×10^{-14}	170	0.0245
40	3.4659×10^{-11}	130	0.0240	7.0070×10^{-14}	170	0.0527
60	4.2485×10^{-11}	130	0.0338	1.1025×10^{-13}	170	0.0606
80	4.8974×10^{-11}	130	0.0423	3.3339×10^{-13}	170	0.0832
100	5.5316×10^{-11}	130	0.0544	9.4581×10^{-13}	170	0.1623

Table 9: Maximum errors of methods for Problem 4 using $h = 0.1$.

Table 8 presents the absolute errors for OSHBM1 and OSHBM2 at the collocation point $N = 20$ for Problem 4. The number of function evaluations (NFE) and CPU time for each method are also included. It can be observed that OSHBM2 consistently achieves lower errors.
Table 9 provides the maximum errors of both OSHBM1 and OSHBM2 at varying collocation points N. As N increases, the CPU time increases correspondingly. Figure 8 offers a graphical comparison of the error performance of OSHBM1 and OSHBM2 for Problem 4 with $h = 0.1$.

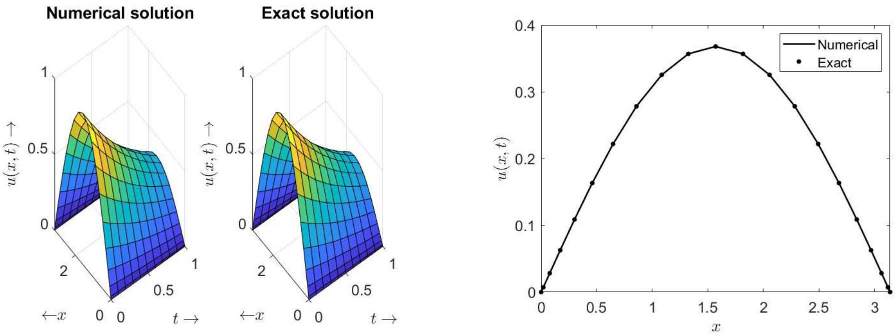

(a) Numerical vs Exact **(b)** Solution profile of OSHBM1&2

Fig. 9: Solution graph for Problem 4.

6 Conclusion

In this paper, we developed optimized spectral hybrid block methods (OSHBMs) for the direct solution of PDEs, where the time variable t is treated using the hybrid block method and the spatial variable x is handled via the spectral collocation method. These methods were derived using an optimization approach and have been shown to be zero-stable, consistent, A-stable, and convergent.

The implementation was carried out using a linear partitioning iterative scheme. The OSHBM1 and OSHBM2 methods produced numerical solutions that closely matched the exact solutions for Problems 1–4, as shown in Figures 3, 4, 7a, and 9a, respectively. The main advantage of the proposed methods is their superior accuracy compared with those in [5] and [15]. Another notable advantage is that they maintain accuracy even for large step sizes (h), whereas the methods in [5] and [15] become less accurate, as evidenced in Tables 4–5 and Figures 2 and 5. This characteristic aligns with the fundamental goal of numerical analysts—to achieve stability and accuracy for a wide range of step sizes. However, a minor drawback of the new methods is that they exhibit fewer significant digits of accuracy than those in [5] and [15] when applied to problems with very small values of h. Overall, the results in Tables 4–9 and Figures 2–9 indicate that the proposed methods are highly efficient and accurate, making them competitive with established numerical techniques.

Declarations

Competing interests: The authors declare that they have no conflicts of interest regarding the publication of this article.
Authors' contributions: All authors contributed equally to this work.
Funding: No funding was received for this study.
Availability of data and materials: All data supporting the findings of this study are included in the article.
Acknowledgments: The authors sincerely thank their colleagues for their valuable suggestions, which significantly improved the quality of this manuscript.

References

[1] T. K. Akinfe, A. C. Loyinmi, A solitary wave solution to the generalized Burgers-Fisher's equation using an improved differential transform method: A hybrid scheme approach, *Heliyon* **7**(5) (2021), 1–16.

[2] T. A. Biala, S. N. Jator, A boundary value approach for solving three-dimensional elliptic and hyperbolic partial differential equations, *SpringerPlus* **4**(588) (2015), 1–16.
[3] T. A. Biala, S. N. Jator, R. B. Adeniyi, Boundary value methods for second-order PDEs via the Lanczos-Chebyshev reduction technique, *Mathematical Problem in Engineering* (2017), 1–11.
[4] T. A. Biala, S. N. Jator, R. B. Adeniyi, Numerical approximations of second order PDEs by boundary value methods and the method of lines, *Afrika Matematika* **12** (2016), 1–8.
[5] J. R. Cash, Two new finite difference schemes for parabolic equations, *SIAM Journal of Numerical Analysis* **21**(3) (1984), 433–446.
[6] G. G. Dahlquist, A special stability problem for linear multistep methods, *BIT Numerical Mathematics* **3**(1) (1963), 27–43.
[7] E. Kogan, The exact traveling wave solutions of a KPP equation, *Symmetry* **16**(12) (2024), 1–11.
[8] J. D. Lambert, *Numerical Methods for Ordinary Differential Systems*, Wiley, New York, (1991).
[9] K. O. Lawal, Y. A. Yahaya, S. D. Yakubu, Four-step block method for solving third-order ordinary differential equations, *International Journal of Mathematics Trends Technology* **57**(5) (2018), 331–344.
[10] S. Liu, Y. Ge, F. Tian, A sixth-order finite difference method for solving the generalized Burgers-Fisher and generalized Burgers-Huxley equations, *ScienceAsia* **49**(5) (2023), 693–702.
[11] J. Lu, G. Yu-Cui, X. Shu-Jiang, Some new exact solutions to the Burgers–Fisher equation and generalized Burgers–Fisher equation, *Chinese Physics* **16**(9) (2007), 2515–2522.
[12] S. Motsa, S. Ahmedai, M. Nefale, O. Otegbeye, A rational optimal block hybrid method for enhanced accuracy in solving Lane–Emden equations, *Partial Differential Equation in Applied Mathematics* **12** (2024), 1–9.
[13] S. S. Motsa, A new spectral local linearization method for nonlinear boundary layer flow problems, *Journal of Applied Mathematics* (2013), 1–15.
[14] S. S. Motsa, V. M. Magagula, P. Sibanda, A bivariate Chebyshev spectral collocation quasilinearization method for nonlinear evolution parabolic equations, *Science World Journal* (2014), 1–13.
[15] F. F. Ngwane, S. N. Jator, L-stable block hybrid second derivative algorithm for parabolic partial differential equations, *America Journal of Computational Mathematics* **4**(2) (2014), 87–92.
[16] M. Rahman, *Mathematical Methods with Applications*, WIT Press, Southampton, (2000).
[17] H. Ramos, M. A. Rufai, An adaptive one-point second-derivative Lobatto-type hybrid method for solving efficiently differential systems, *International Journal of Computational Mathematics* **99**(8) (2022), 1687–1705.
[18] H. Ramos, M. A. Rufai, A new one-step method with three intermediate points in a variable step-size mode for stiff differential systems, *Journal of Mathematics and Chemistry* (2022), 1–16.
[19] J. Sunday, C. Chigozie, E. O. Omole, J. B. Gwong, A pair of three-step hybrid block methods for the solutions of linear and nonlinear first-order systems, *European Journal of Mathematics and Statistics* **3**(1) (2022), 14–25.
[20] L. N. Trefethen, *Spectral Methods in MATLAB*, SIAM, Philadelphia, (2000).
[21] P. Jena,, A. K. Pati, Development of conformable fractional numerical methods of constant order using fractional power series theorem, *Jordan Journal of Mathematics and Statistics* **18**(2) (2025), 233–241.
[22] N. K. Wadhawan, Numerical approximation of Lambert W function for real values by unique method of quadratic approximation, *Jordan Journal of Mathematics and Statistics* **18**(2) (2022), 285–315.